

## SUPPLEMENTAL MATERIAL

### Quantum Hall ferromagnets and transport properties of buckled Dirac materials

Wenchen Luo and Tapash Chakraborty

*Department of Physics and Astronomy, University of Manitoba, Winnipeg, Canada R3T 2N2*

(Dated: June 29, 2015)

#### I. MANY-BODY HAMILTONIAN OF GENERIC DIRAC MATERIALS WITH BUCKLING

In a generic two-dimensional (2D) Dirac material with buckling, the eigen wave functions are given by Eq. (2) in the letter. We divide the wavefunctions into those for two pseudo-layers between which there is a separation  $d$ . The electrons essentially belong to a double-layer system. Using the density matrix defined in Eq. (3) in the letter, the many-body Hamiltonian in the Hartree-Fock approximation (HFA) is given by

$$\begin{aligned}
H = & \sum_{\sigma} \left( E_{\sigma} + \frac{e^2}{\kappa \ell} \frac{d}{2\ell} \sum_{\sigma'} y_{\sigma'} \langle \rho_{\sigma', \sigma'}(0) \rangle y_{\sigma} \right) \rho_{\sigma, \sigma}(0) \\
& + \frac{e^2}{\kappa \ell} \sum_{\sigma, \sigma'} \overline{\sum_{\mathbf{q}}} H_{\eta, \eta'}(\mathbf{q}) \langle \rho_{\sigma, \sigma}(-\mathbf{q}) \rangle \rho_{\sigma', \sigma'}(\mathbf{q}) \\
& - \frac{e^2}{\kappa \ell} \sum_{\sigma, \sigma'} \sum_{\mathbf{q}} X_{\eta, \eta'}(\mathbf{q}) \langle \rho_{\sigma, \sigma'}(-\mathbf{q}) \rangle \rho_{\sigma', \sigma}(\mathbf{q}), \tag{1}
\end{aligned}$$

where  $\kappa$  is the dielectric constant,  $\sigma, \sigma' = 1 \rightarrow (K, \uparrow), 2 \rightarrow (K, \downarrow), 3 \rightarrow (K', \uparrow), 4 \rightarrow (K', \downarrow)$  are the valley-spin indices,  $\eta$  and  $\eta'$  are the valley indices in  $\sigma$  and  $\sigma'$  respectively, and  $y_1 = y_2 = a^2, y_3 = y_4 = -b^2$ .  $E_{\sigma}$  is the kinetic energy of level  $\sigma$  with the Zeeman coupling. The summation with a bar excludes the term of  $\mathbf{q} = \mathbf{0}$ . The functions  $H_{\eta, \eta'}$  and  $X_{\eta, \eta'}$  describe the Hartree and Fock interactions between valleys  $\eta$  and  $\eta'$ ,

$$H_{\eta, \eta'}(\mathbf{q}) = \frac{1}{q\ell} \xi_{\eta, \eta'}(q\ell), \tag{2}$$

$$X_{\eta, \eta'}(\mathbf{q}) = \int_0^{\infty} dp J_0(pq\ell) \xi_{\eta, \eta'}(p), \tag{3}$$

where  $J$  is the Bessel function and

$$\xi_{\eta, \eta} = a^4 f_{n, n} + b^4 f_{n-1, n-1} + 2a^2 b^2 f_{n, n-1} e^{-qd/\ell}, \tag{4}$$

$$\xi_{\eta, \bar{\eta}} = (a^4 f_{n, n} + b^4 f_{n-1, n-1}) e^{-qd/\ell} + 2a^2 b^2 f_{n, n-1}, \tag{5}$$

with  $\bar{\eta}$  being the valley other than  $\eta$ . The function  $f$  is

$$f_{n, m}(q) = e^{-q^2/2} L_n(q^2/2) L_m(q^2/2), \tag{6}$$

with a Laguerre polynomial  $L_n$  ( $L_{n < 0} = 0$ ).

For a liquid phase at quarter filling of a Landau level the ground state is polarized. The nonzero density matrix elements give the distribution of electrons  $\langle \rho_{1,1}(0) \rangle, \langle \rho_{3,3}(0) \rangle$  and the coherence  $\langle \rho_{1,3}(0) \rangle, \langle \rho_{3,1}(0) \rangle$

$$\langle \rho_{1,1}(0) \rangle + \langle \rho_{3,3}(0) \rangle = 1, \tag{7}$$

$$\langle \rho_{1,3}(0) \rangle = \langle \rho_{3,1}(0) \rangle = \sqrt{\langle \rho_{1,1}(0) \rangle \langle \rho_{3,3}(0) \rangle}, \tag{8}$$

where we choose all order parameters to be real. Hence, the energy is given by

$$\begin{aligned}
E = & \sum_{\sigma=1,3} \left( E_{\sigma} + \frac{e^2}{\kappa \ell} \frac{d}{\ell} \sum_{\sigma'=1,3} y_{\sigma'} \langle \rho_{\sigma', \sigma'}(0) \rangle y_{\sigma} \right) \langle \rho_{\sigma, \sigma}(0) \rangle \\
& - \frac{e^2}{\kappa \ell} \sum_{\sigma, \sigma'=1,3} X_{\eta, \eta'}(\mathbf{0}) \langle \rho_{\sigma, \sigma'}(0) \rangle \rho_{\sigma', \sigma}(0). \tag{9}
\end{aligned}$$

By using the conditions  $X_{K,K'} = X_{K',K}$ ,  $X_{K,K} = X_{K',K'}$  and ignoring the constant kinetic energy, we obtain

$$E = 2 \frac{e^2}{\kappa \ell} \left[ (a^2 - b^2)^2 d/\ell - X_{K,K}(\mathbf{0}) + X_{K,K'}(\mathbf{0}) \right] \langle \rho_{1,1}(0) \rangle (\langle \rho_{1,1}(0) \rangle - 1). \quad (10)$$

## II. MANY-BODY HAMILTONIAN OF SILICENE

The elements of the density matrix with extra orbital index can be obtained by modifying Eq. (3) in the letter:

$$\rho_{\alpha,o;\beta,\sigma'}(\mathbf{q}) = \frac{1}{N_\phi} \sum_{X_1, X_2} e^{-\frac{i}{2} q_x (X_1 + X_2)} \delta_{X_1, X_2 + q_y \ell^2} c_{\alpha,o,X_1}^\dagger c_{\beta,\sigma',X_2}, \quad (11)$$

where  $\alpha, \beta$  are valley indices,  $o, o'$  are orbital indices. Since the orbitals are not conserved the many-body Hamiltonian in the HFA is more complex than that in Eq. (1),

$$\begin{aligned} H = & \frac{e^2}{\kappa \ell} \sum_{\alpha,o} \tilde{E}_{\alpha,o} \rho_{\alpha,o;\alpha,o}(0) \\ & + \frac{e^2}{\kappa \ell} \sum_{\alpha,\beta} \sum_{o_1, \dots, o_4} \overline{\sum_{\mathbf{q}} H_{o_1, o_2, o_3, o_4}^{\alpha, \beta}(\mathbf{q})} \langle \rho_{\alpha, o_1; \alpha, o_2}(-\mathbf{q}) \rangle \rho_{\beta, o_3; \beta, o_4}(\mathbf{q}) \\ & - \frac{e^2}{\kappa \ell} \sum_{\alpha,\beta} \sum_{o_1, \dots, o_4} \sum_{\mathbf{q}} X_{o_1, o_4, o_3, o_2}^{\alpha, \beta}(\mathbf{q}) \langle \rho_{\alpha, o_1; \alpha, o_2}(-\mathbf{q}) \rangle \rho_{\beta, o_3; \beta, o_4}(\mathbf{q}), \end{aligned} \quad (12)$$

where  $\tilde{E}_{\alpha,o}$  contains the kinetic energy  $E_{\alpha,o}$  of the orbital  $o$  in valley  $\alpha$  and a capacitive energy,

$$\tilde{E}_{\alpha,o} = E_{\alpha,o} + \frac{d}{\ell} \left[ \frac{\nu}{2} - \sum_{\beta, o'} U_{\alpha, o; \beta, o'}^0 \langle \rho_{\beta, o'; \beta, o'}(0) \rangle \right], \quad (13)$$

$$U_{\alpha, o; \beta, o'}^0 = \left( \sum_{i=1,3} \sum_{j=2,4} + \sum_{i=2,4} \sum_{j=1,3} \right) |c_{o,i}^\alpha|^2 |c_{o',j}^\beta|^2, \quad (14)$$

with the filling factor  $\nu$ . The Hartree interaction is

$$\begin{aligned} H_{o_1, o_2, o_3, o_4}^{\alpha, \beta}(\mathbf{q}) = & \sum_{m,n=1}^2 \sum_{i=m, m+2} \sum_{j=n, n+2} G_{1,2,3,4}^{\alpha, \beta; i, j} P_{m,n}(q\ell) \\ & \times \frac{F_{1,2,3,4}}{q\ell} \Theta_{o_1 + \alpha_i, o_2 + \alpha_i}(q\ell) \Theta_{o_3 + \beta_j, o_4 + \beta_j}(q\ell) \end{aligned} \quad (15)$$

where we define a function  $P_{m,n}(q) = e^{-|m-n|qd/\ell - q^2/2}$  and coefficients

$$G_{1,2,3,4}^{\alpha, \beta; i, j} = c_{o_1, i}^{\alpha*} c_{o_2, i}^\alpha c_{o_3, j}^{\beta*} c_{o_4, j}^\beta, \quad (16)$$

$$F_{1,2,3,4} = e^{-i(o_1 - o_2)\theta} e^{-i(o_3 - o_4)(\theta + \pi)}, \quad (17)$$

with the angle  $\theta$  between vector  $\mathbf{q}$  and  $x$  axis. Function  $\Theta$  is defined as

$$\Theta_{k,l}(p) = \frac{\sqrt{\min(k,l)!}}{\sqrt{\max(k,l)!}} \frac{(ip)^{|k-l|}}{\sqrt{2}^{|k-l|}} L_{\min(k,l)}^{|k-l|} \left( \frac{p^2}{2} \right). \quad (18)$$

The Fock interaction is

$$\begin{aligned} X_{o_1, o_4, o_3, o_2}^{\alpha, \beta}(\mathbf{q}) = & \sum_{m,n=1}^2 \sum_{i=m, m+2} \sum_{j=n, n+2} G_{1,4,3,2}^{\alpha, \beta; i, j} \int dp P_{m,n}(p) \\ & \times \Theta_{o_1 + \alpha_i, o_4 + \alpha_i}(p) \Theta_{o_3 + \beta_j, o_2 + \beta_j}(-p) J_{o_1 - o_4 + o_3 - o_2}(pq\ell). \end{aligned} \quad (19)$$

Once we obtain the HF Hamiltonian, we could obtain the order parameters of the ground state by solving the equation of motion of the single Green's function<sup>1</sup>.

### III. PSEUDO-SPIN STIFFNESS OF THE ANISOTROPIC NONLINEAR $\sigma$ MODEL

We extract the Fock energy functional from the Hamiltonian,

$$H_F = -\frac{e^2}{\kappa\ell} \sum_{\alpha,\beta} \sum_{o_1,o_2,o_3,o_4} \sum_{\mathbf{q}} X_{o_1,o_4,o_3,o_2}^{\alpha,\beta}(\mathbf{q}) \langle \rho_{\alpha,o_1;\beta,o_2}(-\mathbf{q}) \rangle \rho_{\beta,o_3;\alpha,o_4}(\mathbf{q}), \quad (20)$$

where we neglect the kinetic energy, the capacitive energy and the Hartree interaction. This is because the kinetic energy is a constant, capacitive energy is very small, and the Hartree term is zero in the slow varying density approximation.

This field theory is only valid when  $E_z = 0$ . If  $E_z \neq 0$ , then the ground state is no longer an easy-plane QHF. The ground state will be valley polarized very rapidly, i.e. the  $E_z$  is very small to polarize the valley pseudo-spin. In the finite  $E_z$  case, the best way is to calculate the microscopic Hamiltonian in the symmetric gauge.

If we consider the two valleys only in orbital  $o = N$ , then the orbital index could be neglected, and

$$\mathcal{E}_F = -\frac{1}{2} \frac{e^2}{\kappa\ell} \sum_{\alpha,\beta} \sum_{\mathbf{q}} X_{N,N,N,N}^{\alpha,\beta}(\mathbf{q}) \langle \rho_{\alpha,\beta}(-\mathbf{q}) \rangle \langle \rho_{\beta,\alpha}(\mathbf{q}) \rangle. \quad (21)$$

Then the Lagrangian of the anisotropic Nonlinear  $\sigma$  model is obtained by calculating the excitation energy when the density matrix is slowly varied<sup>2</sup>,

$$L = \frac{1}{2} \sum_{\mu=x,y,z} \rho_{\mu} (\partial_{\mu} m_{\mu})^2, \quad (22)$$

where the normalized pseudo-spin field  $\mathbf{m}$  is defined by

$$m_x(\mathbf{r}) + im_y(\mathbf{r}) = 4\pi\ell^2 \langle \rho_{K,K'}(\mathbf{r}) \rangle, \quad (23)$$

$$m_z(\mathbf{r}) = 4\pi\ell^2 (\langle \rho_{K,K}(\mathbf{r}) \rangle - \langle \rho_{K',K'}(\mathbf{r}) \rangle), \quad (24)$$

and the pseudo-spin stiffnesses are given by

$$\rho_z = -\frac{1}{8\pi\ell^2} \lim_{q \rightarrow 0} \nabla_q^2 X_{N,N,N,N}^{K,K}(\mathbf{q}), \quad (25)$$

$$\rho_x = \rho_y = -\frac{1}{8\pi\ell^2} \lim_{q \rightarrow 0} \nabla_q^2 X_{N,N,N,N}^{K,K'}(\mathbf{q}). \quad (26)$$

The excitation energy of a bimeron or an anti-bimeron is

$$\delta E = \frac{4\pi}{3} (\rho_x + \rho_y + \rho_z). \quad (27)$$

Note that this energy which is obtained in the field theory is not identical to a single charged excitation of the electron gas. However, the excitation energy of a bimeron-antibimeron pair in the field theory is identical to that in the electron gas, which is double of  $\delta E$ ,

$$\delta E_{pair} = \frac{8\pi}{3} (\rho_x + \rho_y + \rho_z). \quad (28)$$

This energy is related to the transport property of the system, which can be measured in a transport experiment.

---

<sup>1</sup> R. Côté and A. H. MacDonald, Phys. Rev. Lett. **65**, 2662 (1990); Phys. Rev. B **44**, 8759 (1991).

<sup>2</sup> K. Moon, H. Mori, Kun Yang, S. M. Girvin, A. H. MacDonald, L. Zheng, D. Yoshioka, and Shou-Cheng Zhang, Phys. Rev. B **51**, 5138 (1995).

# Quantum Hall ferromagnets and transport properties of buckled Dirac materials

Wenchen Luo and Tapash Chakraborty

*Department of Physics and Astronomy, University of Manitoba, Winnipeg, Canada R3T 2N2*

(Dated: June 29, 2015)

We study the ground states and low-energy excitations of a generic Dirac material with spin-orbit coupling and a buckling structure in the presence of a perpendicular magnetic field. The ground states can be classified into three types under different conditions: SU(2), easy-plane, and Ising quantum Hall ferromagnets. For the SU(2) and the easy-plane quantum Hall ferromagnets there are goldstone modes in the collective excitations, while all the modes are gapped in an Ising-type ground state. We compare the Ising quantum Hall ferromagnet with that of bilayer graphene and present the domain wall solution at finite temperatures. We then specify the phase transitions and transport gaps in silicene in Landau levels 0 and 1. The phase diagram strongly depends on the magnetic field and the dielectric constant. We note that there exists triple points in the phase diagrams in Landau level  $N = 1$  that could be observed in experiments.

Recently, several graphene-like systems such as silicene, germanene [1] and transition metal dichalcogenides (MoS<sub>2</sub>) [2] have received considerable attention. They all have a honeycomb geometry in the  $xy$  plane as in graphene [3, 4], but additionally with a buckled structure in the  $z$  direction. The buckling is induced by the atoms that are heavier than the carbon atoms in graphene. The heavy atoms also have more complex electron orbitals. In these systems the spin-orbit (SO) coupling is important, while the SO coupling is negligible in graphene. Hence, the electrons in these systems must be described by a massive Dirac equation in which the mass is induced by the SO coupling. We generically call these materials as buckled Dirac materials. The Brillouin zone is similar to that of graphene: a hexagon with two inequivalent valleys  $K$  and  $K'$ . In MoS<sub>2</sub> the  $\Gamma$  point is important because the energy near this point is close to that in the  $K, K'$  valleys in the valence band. For simplicity, in this paper, we consider only the  $K$  and  $K'$  valleys in order to compare with graphene.

In the presence of an applied perpendicular magnetic field the electron bands split into a series of Landau levels (LLs) near the two valleys. The fractional quantum Hall (QH) effect [5] has been studied recently in silicene and germanene [6]. The fractal butterflies have also been investigated theoretically in these systems [7]. Here we report on the ground states and transport properties of the symmetry broken states in the integer QH effect regime. In bilayer and multilayer graphene [9, 10], earlier theoretical works have indicated that the ground states in the  $N \neq 0$  LLs are Ising quantum Hall ferromagnets (QHF), since the interlayer Coulomb potential is different from the intralayer one. The resulting transport properties of bilayer graphene were also observed in an experiment [11]. In buckled Dirac materials the buckling divides the system into two “pseudo-layers”. Atoms  $A$  and  $B$  belong to different pseudo-layers, respectively. Hence the buckling structure makes these monolayer Dirac materials similar to bilayer graphene, i.e., we could observe the Ising QHF in these one-atom-layer systems. We discuss below the various QH states and the collective modes of different QHFs in a few LLs.

The buckling also couples to an external electric field. Without the magnetic field, silicene and germanene may be converted to topological insulators in an appropriate electric field [12]. In the QH regime the phases and transport properties are also much richer and more interesting when the electric field is applied. In this work, we will specifically discuss how the electric field and the dielectric constant (of different substrates) change the phase diagram and control the spin and valley pseudo-spin in silicene. These materials are therefore potential candidates for application in spintronics.

We first consider a generic monolayer Dirac material with the SO coupling. The Brillouin zone is in general a regular hexagon (as in graphene) with two inequivalent valleys  $K$  and  $K'$ . The noninteracting Hamiltonian around valley  $\eta = K, K'$  in a magnetic field is

$$H_\eta = v_F (\sigma_x P_x - \eta \sigma_y P_y) - \lambda_{SO} \sigma_z, \quad (1)$$

where  $\eta = 1, -1$  for the  $K$  and  $K'$  valley respectively,  $v_F$  is the Fermi velocity,  $\sigma$  is the Pauli matrix,  $\mathbf{P} = \mathbf{p} + e\mathbf{A}$  is the canonical momentum and  $\lambda_{SO}$  describes the SO coupling parameter. The SO strength is also described as the mass of the Dirac fermion near each valley. We choose the Landau gauge of the vector potential  $\mathbf{A} = (0, Bx, 0)$ . The LL energy spectrum is given by  $E_0 = \pm \lambda_{SO}$  and  $E_{n \neq 0} = \text{sgn}(n) \sqrt{\lambda_{SO}^2 + 2(v_F \hbar / \ell)^2 \sqrt{n^2 + |n|}}$ , where  $\ell = \sqrt{\hbar / eB}$  is the magnetic length and  $n$  is the LL index. The eigen wavefunctions in the two valleys are

$$\psi_{n,X}^K = \begin{pmatrix} \tilde{a} h_{n,X} \\ \tilde{b} h_{n-1,X} \end{pmatrix}, \psi_{n,X}^{K'} = \begin{pmatrix} \tilde{b} h_{n-1,X} \\ \tilde{a} h_{n,X} \end{pmatrix}, \quad (2)$$

where  $X$  is the guiding center,  $h_{n,X}$  ( $h_{n < 0} = 0$ ) is the LL wave function of a two-dimensional electron gas (2DEG) in a conventional semiconductor. We define  $a = |\tilde{a}|$ ,  $b = |\tilde{b}|$ , so the normalization condition is  $a^2 + b^2 = 1$ . In MoS<sub>2</sub> the  $\Gamma$  point should be included in the Hamiltonian. The low-energy effective Hamiltonian is due to the three  $d$ -orbitals of Mo atoms which are located in the same plane [8]. So the MoS<sub>2</sub> is equivalent to a monolayer system without buckling.

If the geometry of the monolayer Dirac material is exactly the same as graphene then the valley pseudo-spin has a SU(2) symmetry in any LL. However, we need to consider the buckling when we calculate the Coulomb interaction. The ground states of bilayer or multi-layer graphene in the  $N \neq 0$  LL are valley pseudo-spin Ising QHFs [9, 10]. The SU(2) symmetry of valley pseudo-spin is broken to a  $Z_2$  symmetry because there is a factor  $e^{-qd}$  difference between the inter-layer and intra-layer Coulomb potentials, where  $q$  is the momentum and  $d$  is the distance between two layers. We follow the formalism in [9, 10] to present a more general classification of the QHFs of the ground states in a buckled Dirac material. We assume a buckling  $d$  in the  $z$  direction between the two elements of the wavefunction spinors in Eq. (2). The buckling divides the wavefunctions into two pseudo-layers. The density matrix  $\rho$  in the momentum space is

$$\rho_{\sigma,\sigma'}(\mathbf{q}) = \frac{1}{N_\phi} \sum_{X_1, X_2} e^{-\frac{i}{2}q_x(X_1+X_2)} \delta_{X_1, X_2+q_y \ell^2} c_{\sigma, X_1}^\dagger c_{\sigma', X_2}, \quad (3)$$

where  $\sigma, \sigma' = 1 \rightarrow (K, \uparrow), 2 \rightarrow (K, \downarrow), 3 \rightarrow (K', \uparrow), 4 \rightarrow (K', \downarrow)$  are the valley-spin indices, the LL degeneracy is  $N_\phi$ , and the creation and annihilation operators of electrons are  $c^\dagger, c$ . The average values of the elements of the density matrix fully describe the system with the Hamiltonian in the Hartree-Fock approximation (HFA) [13].

For a quarter filling of a LL which is equivalent to the case of three-quarter filling due to the electron-hole symmetry, the ground state satisfies  $\langle \rho_{1,1}(0) \rangle + \langle \rho_{3,3}(0) \rangle = 1$ . The energy of the liquid phase, without a constant, is given by  $E = 2Q \langle \rho_{1,1}(0) \rangle (\langle \rho_{1,1}(0) \rangle - 1) e^2 / \kappa \ell$ , where  $\kappa$  is dielectric constant, and

$$\tilde{Q}(\mathbf{q}) = (a^2 - b^2)^2 d / \ell - X_{K,K}(\mathbf{q}) + X_{K,K'}(\mathbf{q}), \quad (4)$$

and  $Q \equiv \tilde{Q}(\mathbf{q} = \mathbf{0})$ . The first term in Eq. (4) is the capacitive energy. The Fock interaction functions  $X_{K,K}(\mathbf{q})$  and  $X_{K,K'}(\mathbf{q})$  are given by Eq. (3) in [13]. We can classify the ground states as follows. If  $Q = 0$ , the ground state is a SU(2) QHF, since  $\langle \rho_{1,1}(0) \rangle$  and  $\langle \rho_{3,3}(0) \rangle$  could be of any value to minimize the energy. If  $Q < 0$ , the ground state is an Ising QHF. The energy is minimized when  $\langle \rho_{1,1}(0) \rangle$  is either 0 or 1. Finally, if  $Q > 0$  the ground state is an easy-plane QHF, i.e., the energy is minimum only when  $\langle \rho_{1,1}(0) \rangle = \langle \rho_{3,3}(0) \rangle = 1/2$ .

We define the two-particle Green's function

$$\chi_{\sigma,\sigma',\gamma,\gamma'}(\mathbf{q}, \mathbf{q}'; \tau_1 - \tau_3) = N_\phi \langle \rho_{\sigma,\sigma'}(\mathbf{q}) \rangle \langle \rho_{\gamma,\gamma'}(-\mathbf{q}') \rangle - N_\phi \langle T \rho_{\sigma,\sigma'}(\mathbf{q}, \tau_1) \rho_{\gamma,\gamma'}(-\mathbf{q}', \tau_3) \rangle,$$

where  $T$  is the time order operator to study the collective behavior of the system. We employ the generalized random phase approximation (GRPA) to solve the equation of motion of the two-particle Green's function. Details can be found in [14, 15]. The non-zero lowest-energy collective mode which is given

by the poles of the retarded Green's functions is  $C(\mathbf{q} \rightarrow \mathbf{0}) = \frac{e^2}{\kappa \ell} |Q [\langle \rho_{1,1}(0) \rangle - \langle \rho_{3,3}(0) \rangle]|$ , which for small  $q$ ,  $C(\mathbf{q}) \sim q^2$ . This collective mode, which is similar to that of an easy-plane QHF in a double quantum well system without tunnelling, is a precess mode of the valley pseudo-spin in the  $xy$  plane [14, 16]. In the three types of QHFs, when  $\mathbf{q} \rightarrow \mathbf{0}$ , the collective modes are distinguished by their gaps. In a SU(2) QHF,  $Q = 0$ , so  $C(\mathbf{q} \rightarrow \mathbf{0}) = 0$ . It is a goldstone mode. In an easy-plane QHF,  $\langle \rho_{1,1}(0) \rangle - \langle \rho_{3,3}(0) \rangle = 0$ , so  $C(\mathbf{q} \rightarrow \mathbf{0}) = 0$ , which means a goldstone mode still exists. In an Ising QHF,  $Q \neq 0$  and  $|\langle \rho_{1,1}(0) \rangle - \langle \rho_{3,3}(0) \rangle| = 1$ . The goldstone mode disappears and all modes are gapped.

We now consider the two actual materials, silicene and germanene, in a perpendicular electric field  $E_z$ . The electric field can control the phases and the spin polarization, useful for application in spintronics or valley pseudo-spintronics. The low-energy noninteracting Hamiltonian, in the basis  $\{A \uparrow, B \uparrow, A \downarrow, B \downarrow\}$  is [17]

$$H_\eta = v_F (p_x \tau_x - \eta p_y \tau_y) + \eta \tau_z h + d E_z \tau_z / 2, \quad (5)$$

where  $h = -\lambda_{SO} \sigma_z - a_0 \lambda_R (p_y \sigma_x - p_x \sigma_y)$ ,  $\eta = 1$  for valley  $K$  and  $-1$  for the  $K'$  valley,  $\tau$  and  $\sigma$  are the Pauli matrices corresponding to the sublattices and the spin,  $a_0$  is the lattice constant,  $\lambda_R$  is the Rashba SO (RSO) coupling and the buckling is  $d$ . For silicene (germanene) [18, 19], these parameters are  $v_F = 5.5 \times 10^5$  ( $5.09 \times 10^5$ ) m/s,  $a_0 = 3.86$  (4.06) Å,  $\lambda_{SO} = 3.9$  (43) meV,  $\lambda_R = 0.7$  (10.7) meV and  $d = 0.46$  (0.66) Å.

The Hamiltonian in Eq. (5) is more complex than that in Eq. (1) since the electric field and the RSO coupling are included. In the QH the wave function in valley  $\alpha$  and orbital  $o$  is  $(c_{o,1}^\alpha h_{o+\alpha_1} \ c_{o,2}^\alpha h_{o+\alpha_2} \ c_{o,3}^\alpha h_{o+\alpha_3} \ c_{o,4}^\alpha h_{o+\alpha_4})^T$ , with the normalization condition  $\sum_{i=1}^4 |c_{o,i}^\alpha|^2 = 1$ , where  $K_1 = K_4 = 0, K_2 = -1, K_3 = 1; K'_1 = -1, K'_2 = K'_3 = 0, K'_4 = 1$ . Because of the RSO coupling the eigenvectors are not spin polarized. We introduce another degree of freedom, the orbital, to replace the spin. We find that without Zeeman coupling the energies of the orbitals  $o = N, N-1$  are close to each other in the LL  $N$ . The concept of the orbital degree of freedom here is similar to that in the  $N = 0$  LL in bilayer graphene. The RSO interaction couples different spins in a valley. For zero RSO coupling the orbital degree of freedom is identical to spin. In reality,  $|c_{N-1,1}^\alpha|, |c_{N-1,2}^\alpha|, |c_{N,3}^\alpha|, |c_{N,4}^\alpha| \lesssim 10^{-4}$ , and so approximately, the orbital  $N$  is associated with spin up and orbital  $N-1$  is associated with spin down. Note that the coefficients  $c_{o,i}^\alpha$  not only depend on the magnetic field but also on the electric field.

We neglect the LL mixing since the LL gap is large ( $E_{N=0} \sim 0, E_{N=\pm 1} \approx \pm 60$  meV for silicene). The density matrix and the many-body Hamiltonian in the HFA are given in [13]. We define the Green's function  $G_{\alpha,o;\beta,o'}(X, X', \tau) = -\langle T c_{\alpha,o,X}(\tau) c_{\beta,o',X'}^\dagger(0) \rangle$ , with a relation to the density matrix at zero temperature,  $G_{\alpha,o;\beta,o'}(\mathbf{q}, \tau = 0^-) = \langle \rho_{\beta,o';\alpha,o}(\mathbf{q}) \rangle$ . Solving the equation of motion of the Green's function we could obtain

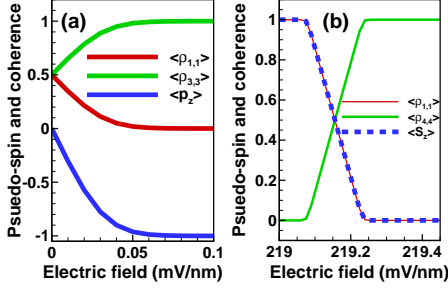


FIG. 1: (Color online) (a) The occupation of the states  $|1\rangle$  and  $|3\rangle$ , and the valley polarization  $\langle p_z \rangle$  at  $\nu = -1$ . (b) Order parameters around the phase transition region at  $\nu = 0$ .

the ground states of the system [20]. In what follows, we define the valley-orbital (or say, valley-spin if  $\lambda_R = 0$ ) indices as  $(K, N) \rightarrow 1, (K, N-1) \rightarrow 2, (K', N) \rightarrow 3, (K', N-1) \rightarrow 4$ , for simplicity.

Due to the electron-hole symmetry, we consider only the quarter- and half-filled LLs. The system can be described in the (pseudo)-spin language. The valley pseudo-spin field in orbital  $o$  is defined by  $p_{o,x} + ip_{o,y} = \langle \rho_{K,o;K',o} \rangle, p_{o,z} = \langle \rho_{K,o;K,o} \rangle - \langle \rho_{K',o;K',o} \rangle$ , and  $\mathbf{p} = \sum_o \mathbf{p}_o$ . We could approximately associate the orbital with the real spin:  $o = N$  associated with spin up and  $o = N-1$  associated with spin down. Hence, we define the spin field:  $S_{\alpha,x} + iS_{\alpha,y} = \langle \rho_{\alpha,N;\alpha,N-1} \rangle, S_{\alpha,z} = \langle \rho_{\alpha,N;\alpha,N} \rangle - \langle \rho_{\alpha,N-1;\alpha,N-1} \rangle$ , and  $\mathbf{S} = \sum_{\alpha} \mathbf{S}_{\alpha}$ .

**Filling factor  $\nu = -1$ :** When  $E_z = 0$ , the ground state is an easy-plane QHF in valley pseudo-spin. It can also be obtained by the classification parameter  $Q$  in Eq. (4):  $Q > 0$  if we approximate  $\lambda_R = 0$ . The ground state lies on the easy-plane QHF regime. It is the symmetric state of the two valleys  $|GS\rangle = (|1\rangle + |3\rangle)/\sqrt{2}$ . When the electric field increases, there is a bias between the two states  $|1\rangle$  and  $|3\rangle$  so that the ground state is a bonding state  $|GS\rangle = a_1|1\rangle + a_3|3\rangle$ . When the electric field is strong  $E_z \gtrsim 0.08$  mV/nm, the bias is large enough to polarize the valley pseudo-spin. The order parameters in the phase transition are shown in Fig. 1 (a).

For an easy-plane QHF, the charged excitation is a bimeron or an anti-bimeron described in the anisotropic nonlinear  $\sigma$  model [21, 22]. At  $E_z = 0$  the Lagrangian of this model can be written as  $L = \frac{1}{2} \sum_{\mu=x,y,z} \rho_{\mu} (\partial_{\mu} m_{\mu})^2$ , where we define the normalized field  $\mathbf{m} = 4\pi\ell^2 \mathbf{p}$ . The pseudo-spin stiffnesses  $\rho_{\mu}$  are defined in Eqs. (25) and (26) in [13]. The excitation energy of a bimeron-antibimeron pair is then given by  $\delta E_{pair} = 8\pi(\rho_x + \rho_y + \rho_z)/3$  [21, 22]. For  $B = 10$  T,  $E_z = 0$ ,  $\kappa = 1$ , the excitation energy of a bimeron-antibimeron pair is 39.2 meV. In comparison, the excitation energy of an electron-hole pair is 156 meV. Hence, the transport gap is due to the bimeron-antibimeron pair.

**Filling factor  $\nu = 0$ :** For  $E_z = 0$ ,  $|1\rangle$  and  $|3\rangle$  are fully occupied, the ground state is spin polarized and

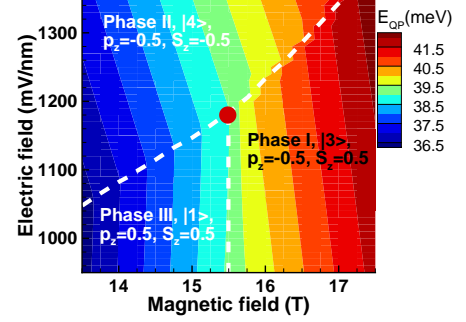


FIG. 2: (Color online) The excitation energy contour of the quasi-particle around the triple point at  $\nu = 3, \kappa = 5$ . The dashed lines are located at the phase transitions. The red dot is the triple point.

is valley unpolarized. The ground state is stable when  $E_z < 219.05$  mV/nm. In the region  $E_z \in [219.05, 219.25]$  mV/nm, the coherence  $\langle \rho_{1,4} \rangle$  between  $|1\rangle$  and  $|4\rangle$  arises. In Fig. 1 (b), we show the phase transition region where  $\langle \rho_{1,1} \rangle$  and  $\langle \rho_{4,4} \rangle$  are gradually changed. The spin of the system is also controlled unpolarized gradually by the electric field. When  $E_z > 219.25$  mV/nm the system is spin unpolarized but valley pseudo-spin polarized, all electrons are in valley  $K'$ .

In the  $N > 0$  LLs the nature of the broken symmetry states are different from those in the  $N = 0$  LL. For  $N > 0$  the ground state of a LL is an Ising QHF, which is similar to bilayer graphene [9, 10]. For simplicity and without loss of generality, we only study the filling factors  $\nu = 3, 4$ , since the LL mixing is important in higher LLs.

**Filling factor  $\nu = 3$ :** For  $E_z = 0$ , we assume that  $\lambda_R = 0$  so that  $Q < 0$ . Hence the ground state is an Ising QHF with a valley  $Z_2$  symmetry, which is also supported by our numerical calculation including  $\lambda_R$ . The  $SU(2)$  valley symmetry is broken to a  $Z_2$  symmetry. Figure 2 shows the phase diagram in a finite electric field for  $\kappa = 5$ . For  $\lambda_R = 0$  the  $SU(2)$  spin symmetry is also broken to a  $Z_2$  symmetry at the phase transition between Phase I (or Phase III) and Phase II. These symmetry broken states are all induced by the small buckling geometry. Note that the valley and spin can also be controlled by the electric or the magnetic field. At the two sides of the phase transition line in Fig. 2, the valley or spin is reversed.

Interestingly, for  $B = 15.5$  T and  $E_z = 1180$  mV/nm, there is a triple point (the red dot in Fig. 2) in the phase diagram. This triple point occurs only when  $\kappa \gtrsim 3$ . When the dielectric constant is very large the electron gas is close to a noninteracting system and the triple point would disappear. At a finite electric field the phase diagram is also changed by the dielectric constant  $\kappa$ . For  $\kappa = 1$  the phase III disappears and only other two phases survive when  $E_z < 2000$  mV/nm.

The Ising QHF here is similar to that in bilayer or multilayer graphene [10], but is different from the Ising QHF

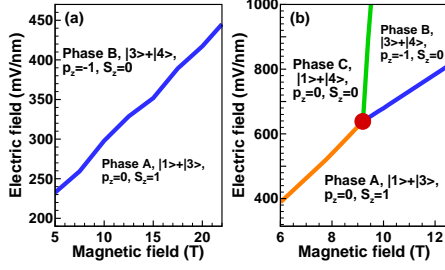


FIG. 3: (Color online) The phase diagrams at  $\nu = 4$  and (a)  $\kappa = 1$ , and (b)  $\kappa = 4$ .

system with different LLs [23] in semiconductor quantum wells. Hence, the lowest charged excitation may be a skyrmion around  $E_z = 0$ . However, the skyrmion in this system must be calculated numerically with a microscopic Hamiltonian in the symmetric gauge.

There is no domain wall at zero temperature. At finite temperature the domain wall could exist to lower the free energy of the system [24], when we consider the wall entropy. Below a critical temperature  $T_C$ , domain walls provide 1D channels carrying extra charges (electron-hole pairs) to dissipate the transport charge of the 2DEG, when the domain walls are dense enough to overlap. So the resistance spike in  $R_{xx}$  appears. Above  $T_C$ , the domain wall will be infinitely long and expand to the sample perimeter. The charge in the domain wall can not dissipate the transport electrons any more and hence the resistance spike disappears. Following the study of the domain wall in a graphene bilayer [10] we obtain the kink domain wall of the valley pseudo-spin at  $E_z = 0$ :  $m_x(\mathbf{r}) = \sin \theta(\mathbf{r})$ ,  $m_y = 0$  and  $m_z(\mathbf{r}) = \cos \theta(\mathbf{r})$  with

$$\theta = 2 \arctan \exp \left[ \sqrt{2(K_z - K_\perp) / \rho_s x} \right], \quad (6)$$

where we approximate  $\rho_s = \rho_x \approx \rho_z$ , and define  $K_\perp = X_{N,N,N,N}^{K,K'}(\mathbf{0}) / (8\pi)$  and  $K_z = X_{N,N,N,N}^{K,K}(\mathbf{0}) / (8\pi)$ . The excitation energy per unit length of the domain wall is then given by  $\delta E = 2\sqrt{2(K_z - K_\perp)\rho_s}$ .

We also present the quasi-particle (QP) excitation energy  $E_{QP}$  around the triple point in Fig. 2. Experimentally, the phase transitions between different spins (Phase I or III to Phase II) can not only be observed in a NMR experiment, but also in a transport measurement. The phase transition between different valleys (Phase I to III) may be observed in a transport or a circular light absorption experiment [25]. At the phase transitions a resistivity spike may be observed due to the existence of the domain wall at finite temperature, which has been reported in a LL Ising QHF [23, 24] and in the Ising QHF of bilayer graphene [10, 11].

*Filling factor  $\nu = 4$ :* For  $\kappa = 1$ , the phase diagram in a magnetic field is shown in Fig. 3 (a). The triple point appears when  $\kappa \gtrsim 3$ . We show an example of the triple point which is marked as a red dot located at  $B = 9.2\text{T}$ ,

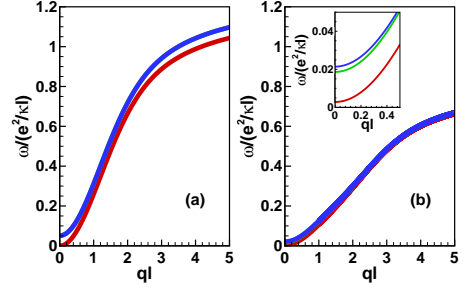


FIG. 4: (Color online) The collective modes for (a) the easy-plane QHF ground state at  $\nu = -1$  and (b) the Ising QHF ground state at  $\nu = 3$ , when  $B = 10\text{T}$ ,  $\kappa = 1$  and  $E_z = 0$ . The small  $q$  region is given as inset.

$E_z = 635\text{mV/nm}$  for  $\kappa = 4$  in Fig. 3 (b). Phase C sets in when  $B < 9.2\text{T}$ , since the kinetic energy contributes more and the Coulomb interaction  $e^2/\kappa\ell$  is decreased by the large dielectric constant.

As we discussed above, the easy-plane QHFs have a goldstone mode while all the modes of Ising QHFs are gapped. In silicene we only show the collective modes at  $\nu = -1$  and 3 in Fig. 4 for simplicity. Note that, in the region  $E_z \in [219.05, 219.25]\text{ mV/nm}$ , the ground state is a bonding state with a goldstone mode at  $\nu = 0$ .

To summarize, we classify the ground states of a generic buckled Dirac material in a magnetic field into three types of QHFs. The low-energy collective modes of the three QHFs are given analytically in the GRPA. A goldstone mode exists in the SU(2) and in the easy-plane QHFs, but not in the Ising QHF. We then focus on a real material, viz., silicene. Without an electric field we note that in silicene the magnetic field is able to change the coefficients  $c_{o,i}^\alpha$  in the wavefunctions. However, in a very small magnetic field ( $B \ll 0.01\text{T}$ ) the ground state becomes an easy-plane QHF at  $\nu = 3$ . In such a low magnetic field the QH effect can not be realized and the LL mixing is not negligible. If the SO coupling can be tuned then the coefficients of wave functions can be modified. For  $B = 10\text{T}$ ,  $\nu = 3$ ,  $\kappa = 1$ , we find that when  $\lambda_{SO} > 750\text{ meV}$ , the ground state at  $\nu = 3$  is an easy-plane QHF. For about  $\lambda_{SO} = 750\text{ meV}$ , the ground state is a SU(2) QHF. This is also true for germanene. If we could efficiently tune the wave function we may realize the phase transition between different QHFs. Experimentally, this transition is observable: the domain wall induced resistivity spike occurs only in an Ising QHF. The phase diagrams and transport properties in the  $N = 0, 1$  LLs in silicene also depend on the magnetic field and the dielectric constant which dramatically change the Coulomb interaction. We have shown the triple points in Figs. 2 and 3. The SU(2) symmetry of the spin and valley are broken by the electric field and the buckling structure. The phase transitions may indeed be observed in NMR, transport or light absorption experiments.

The work has been supported by the Canada Research



Chairs Program of the Government of Canada.

- 
- [1] K. Takeda and K. Shiraishi, Phys. Rev. B **50**, 14916 (1994); C.-C. Liu, W. Feng, and Y. Yao, Phys. Rev. Lett. **107**, 076802 (2011); Y. Wang, J. Zheng, Z. Ni, R. Fei, Q. Liu, R. Quhe, C. Xu, J. Zhou, Z. Gao, and J. Lu, Nano **07**, 1250037 (2012); F.-B. Zheng and C.-W. Zhang, Nanoscale Res. Lett. **7**, 422 (2010); A. Kara, H. Enriquez, A.P. Seitsonen, L.C. Lew Yan Voon, S. Vizzini, B. Aufray, and H. Oughaddou, Surf. Sci. Rep. **67**, 1 (2012); Q. Tang and Z. Zhou Progr. Mater. Sci. **58**, 1244 (2013); H. Rostami, A. Moghaddam, and R. Asgari, Phys. Rev. B **88**, 085440 (2013); A. Kormnyos, V. Zlyomi, N. Drummond, P. Rakyta, G. Burkard, and V. Falko, Phys. Rev. B **88** 045416 (2013).
- [2] Q. H. Wang, K. Kalantar-Zadeh, A. Kis, J. N. Coleman and M. S. Strano, Nature Nanotech. **7**, 699–712 (2012).
- [3] H. Aoki and M.S. Dresselhaus (Eds.), *Physics of Graphene* (Springer, New York 2014).
- [4] D.S.L. Abergel, V. Apalkov, J. Berashevich, K. Ziegler, and T. Chakraborty, Adv. Phys. **59**, 261 (2010).
- [5] T. Chakraborty and V. Apalkov, in [3] Ch. 8; T. Chakraborty and V.M. Apalkov, Solid State Commun. **175**, 123 (2013); T. Chakraborty and P. Pietiläinen, Phys. Rev. Lett. **76**, 4018 (1996); D.S.L. Abergel and T. Chakraborty, *ibid.* **102**, 056807 (2009); V.M. Apalkov and T. Chakraborty, *ibid.* **97**, 126801 (2006); *ibid.* **105**, 036801 (2010); *ibid.* **107**, 186803 (2011).
- [6] V. M. Apalkov and T. Chakraborty, Phys. Rev. B **90**, 245108 (2014).
- [7] V.M. Apalkov and T. Chakraborty, Phys. Rev. B (to be published).
- [8] Z. Y. Zhu, Y. C. Cheng, and U. Schwingenschlögl, Phys. Rev. B **84**, 153402 (2011); G.-B. Liu, W.-Y. Shan, Y. Yao, W. Yao, and D. Xiao *ibid.* **88**, 085433 (2013); J. E. Padilha, H. Peelaers, A. Janotti, and C. G. Van de Walle, *ibid.* **90**, 205420 (2014); Y.-H. Ho, W.-P. Su and M.-F. Lin, RSC Adv. **5**, 20858 (2015).
- [9] W. Luo, R. Côté and A. Bédard-Vallée, Phys. Rev. B **90**, 075425 (2014).
- [10] W. Luo and R. Côté, Phys. Rev. B **90**, 245410 (2014).
- [11] K. Lee, B. Fallahazad, J. Xue, D. C. Dillen, K. Kim, T. Taniguchi, K. Watanabe, and E. Tutuc, Science **345**, 58 (2014).
- [12] M. Tahir and U. Schwingenschlögl, Sci. Rep. **3**, 1075 (2013),
- [13] see the Supplemental Material.
- [14] R. Côté, D. B. Boisvert, J. Bourassa, M. Boissonneault, and H. A. Fertig, Phys. Rev. B **76**, 125320 (2007).
- [15] J. Lambert and R. Côté, Phys. Rev. B **87**, 115415 (2013).
- [16] Z. F. Ezawa, Phys. Rev. Lett. **82**, 3512 (1999); Z. F. Ezawa, Physica B **463**, 294-295 (2001); Z. F. Ezawa and G. Tsitsishvili, Phys. Rev. B **70**, 125304 (2004).
- [17] Z. Ni, Q. Liu, K. Tang, J. Zheng, J. Zhou, R. Qin, Z. Gao, D. Yu, and J. Lu, Nano Lett. **12**, 113 (2012); M. Ezawa, New J. Phys. **14**, 033003 (2012); M. Ezawa, J. Phys. Soc. Jpn, **81**, 064705 (2012).
- [18] C.-C. Liu, H. Jiang, and Y. Yao, Phys. Rev. B **84**, 195430 (2011).
- [19] N. J. Roome and J. D. Carey, ACS Appl. Mater. Interfaces **6**, 7743-7750 (2014).
- [20] R. Côté and A. H. MacDonald, Phys. Rev. Lett. **65**, 2662 (1990); Phys. Rev. B **44**, 8759 (1991).
- [21] K. Moon, H. Mori, Kun Yang, S. M. Girvin, A. H. MacDonald, L. Zheng, D. Yoshioka, and Shou-Cheng Zhang, Phys. Rev. B **51**, 5138 (1995).
- [22] Z.F. Ezawa, *Quantum Hall Effects; Field Theoretical Approach and Related Topics* (World Scientific, Singapore 2008), 2nd edition; Z.F. Ezawa and G. Tsitsishvili, Rep. Prog. Phys. **72**, 086502 (2009).
- [23] A. J. Daneshvar, C. J. B. Ford, M. Y. Simmons, A. V. Khaetskii, A. R. Hamilton, M. Pepper, and D. A. Ritchie, Phys. Rev. Lett. **79**, 4449 (1997); T. Jungwirth, S. P. Shukla, L. Smrčka, M. Shayegan, and A. H. MacDonald, Phys. Rev. Lett. **81**, 2328 (1998); V. Piazza, V. Pellegrini, F. Beltram, W. Wegscheider, T. Jungwirth, and A. H. MacDonald, Nature (London) **402**, 638 (1999).
- [24] T. Jungwirth and A. H. MacDonald, Phys. Rev. Lett. **87**, 216801 (2001); T. Jungwirth and A. H. MacDonald, Phys. Rev. B **63**, 035305 (2000).
- [25] C.J. Tabert and E.J. Nicol, Phys. Rev. Lett. **110**, 197402 (2013).